SWITCHABLE PHOTODETECTOR USING PHASE CHANGE MATERIAL $Ge_2Sb_2Te_5$

A DISSERTATION

Submitted in partial fulfilment of the

requirements for the award of the degree

of

MASTER OF TECHNOLOGY IN PHOTONICS

By

SUYASH KUSHWAHA

Enrolment No. – 17560008

DEPARTMENT OF PHYSICS

INDIAN INSTITUTE OF TECHNOLOGY ROORKEE

ROORKEE-247667 (INDIA)

MAY 2019

Declaration

I hereby declare that the project entitled "**Switchable Photodetector using Phase change material $Ge_2Sb_2Te_5$**" submitted by me to the Department of Physics, IIT Roorkee in partial fulfilment of the requirement for the award of the degree of Master of Technology in Photonics is a record of my own work carried out during the period Jan 2018 to May 2019 under the supervision of Dr. Rajesh Kumar.

Place: Roorkee (SUYASH KUSHWAHA)
Date: M.Tech. Photonics
I.I.T. Roorkee

Certification

This is to certify that the above statement made by the candidate is correct to the best of my knowledge.

Place: Roorkee Dr. Rajesh Kumar
Date: Department of Physics
I.I.T. Roorkee

Acknowledgement

It is a matter of great pleasure to express my gratitude and veneration to Dr. Rajesh Kumar for his valuable supervision, convincing discussions, his constant inspiration throughout this work and for his valuable time he gave to me.

I also wish to thank Head of the Department of Physics for his help.

I am grateful to Mr. Nadir Ali and Mr. Shubham Singh (Research scholars) for their persistent help and discussions they made with me.

I would also like to express my gratitude and respect to my family and friends.

Abstract

This thesis reports the possibility of development of a broader range photodetector which could efficiently work in multiple wavelength ranges from conventional communication band to near infrared band. This device is developed by silicon-on-insulator platform in silicon photonics by using phase change material $Ge_2Sb_2Te_5$ (GST). All the simulations are done in CST microwave studio. Every possible effort has been made at time of designing to optimise important parameters of photodetector device such as, absorption, responsivity, quantum efficiency etc. I have summarized results and analysed some sensitive and non-sensitive parameters.

Index

List of Figures

List of Tables

Unit 1: Introduction

Silicon photonics is the study and making use of photonic systems which uses silicon as an optical medium for movement of photons in an integrated photonic chip or system. It has already been used in the electronics circuitry for many years and now silicon photonics has become an emerging choice in photonics industry. In recent years we have seen many breakthroughs and the increasing investments in international markets, and has become a very important integral discipline in integrated optics.

The motivation for silicon photonics:

Traditional reason: Silicon wafers have

- Lowest manufacturing cost due to abundance in nature.
- Highest crystal quality.

New Insight:

- The abundance of high-quality silicon-on-insulator (SOI) wafers, an ideal platform for creating planar waveguide circuits through which light can easily travel.
- A good optical confinement is also achieved due to high index contrast between silicon & silicon dioxide helps in size scaling.

The use of silicon photonics is not only limited to optical communication systems but it is known to possess linear and nonlinear optical properties in the infrared region also. Also, properties like thermal conductance and its threshold for optical damage have made industry able to produce a reliable class of mid Infrared based photonic devices [1].

These operate in infrared region, most commonly at the 1.55 μm λ, popularly known as communication wavelength [4].

The silicon typically lies on top of a layer of silica are known as silicon on insulator (SOI).

The propagation of light through silicon devices is governed by a range of nonlinear optical phenomena

- Kerr Effect,
- The Raman Effect,
- Interactions between Photons and Free Charge Carriers.

Applications: -

- Spectral Filters and Switches.
- Photodetectors.
- Optical Delay Lines.
- Sensing applications such as Strain Sensor, temperature change, refractive index change.
- Label Free Biosensors
- Using Active Ring Resonator, we can construct Modulator, Hybrid Silicon Rings.

Silicon on Insulator platform

Silicon on Insulator was chosen as the best solution to fit our purposes, due to few reasons told in above paragraph. Silicon behaves transparent to the range of wavelengths extending from 1100 nm to the far infrared region this covers both second and third bandwidth window of the optical communications. The R.I. contrast of Silicon (n_{Si} = 3.5) and Silica (n_{SiO2} = 1.46) is ∇n = 1.4, is a high enough value to get good mode confinement of the optical field in any waveguide made on SOI platform. Typical waveguide cross sections are 220 x 480 nm^2 that is used for good confinement and to make waveguide to support single mode [1].

Only a few nm amplitude scale of roughness is enough to produce much propagation loss. Silicon photonics has attracted interest in the last few years for its compatibility with the CMOS industry. The fabrication process can be carried out in established industrial machines itself to manage the cost of production.

The eventual integration with microelectronics and monolithic photonic integration with other platform would make it possible to realize, on the same substrate, all the optical functionalities and use it in a vision of optical interconnection.

A key limitation for Silicon is the scattering process due to sidewall roughness that becomes the dominant contribution to the losses [2].

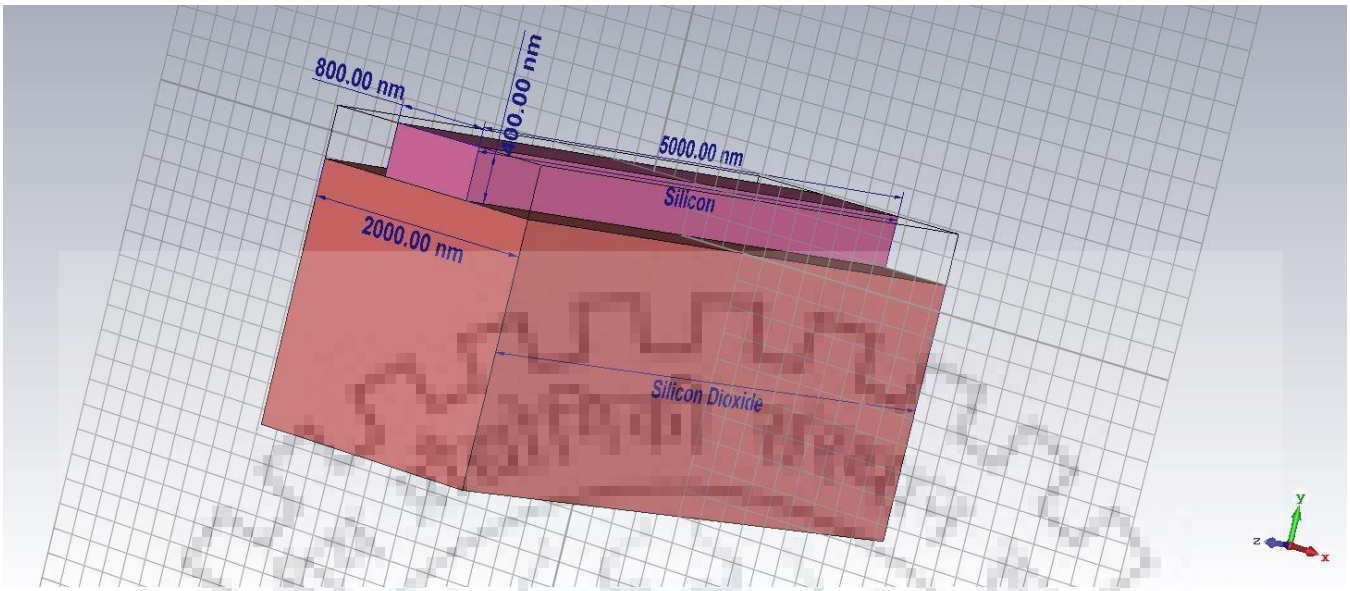

Figure 1 A silicon waveguide on SiO_2 substrate.

Unit 2: Photodetector

Introduction:

Photodetectors or sometimes termed as photoconductors are optoelectronic devices that converts optical energy (light) to suitable electrical parameter i.e. current or voltage. This optical to electrical conversion of energy could be done by selection of suitable device according to the parameter which is most important in our work. Since there are number of detectors available in market, different kind of detectors have some efficient parameters and some redundant parameters depending upon the kind of application in which they are being used. If one of the detectors is being picked up for use then there must be some trade off in between some of its parameters that will be provided in individual sections of photodetectors. Some commonly used detectors are named below:

- Photoconductor
- MSM detector
- P-N junction photodiode
- PIN photodiode
- Avalanche photodiode
- Phototransistor
- Waveguide Photodetectors

Every above mentioned device uses semiconductor material called as active region where photon or light absorption occurs. Before selecting a material and using it as active medium in devices it is very much required that selected material fulfil some optical, electronic and physical properties that are being provided in next section. Some important parameters which plays significant role in selection of active material for photodetector are:

- **Direct Band gap Material**

  A material in which lowest energy level of conduction band and highest energy level of valance band have same value of wave vector k in the energy-momentum diagram of semiconductor material is suitable to be used as active material. A direct band gap material tested from its dispersion diagram is good absorber of photons falling on it. However in indirect band gap materials electron hole pair generation is much more difficult [3].

- **Wavelength region of operation**

  Energy band gap of semiconductor is very useful parameter for photodetector. It defines working region of photodetectors. Material is selected according to wavelength of light source to be detected.

$$Eg \leq h\nu \tag{2.1}$$

  Where, E_g is energy band gap of semiconductor and $h\nu$ is the energy of incident photon on detector. If energy of impinging photon is less than energy band gap of semiconductor then photon is not absorbed and does not result in generation of excess carriers in active region. Also, if energy of incident photon is much more than band gap of material then excited electron gets trapped in deep states and results in reduction of photocurrent [4].

- **Absorption coefficient**

  Absorption coefficient is very crucial factor for a semiconductor to be selected as active material of photodetectors. The absorption coefficient decides the penetration depth of the light falling on the device. Here Beer-Lambert law is used to determine penetration depth. Penetration depth can be calculated as inverse of absorption coefficient. If absorption coefficient, α is very large the maximum absorption would be close to the surface and with small α most of the incident light will pass away through material without absorption.[4]

- **Lesser refractive index contrast with silicon**

  In order to increase the optical to electrical conversion efficiency of device one should minimise the reflection at interface by reducing refractive index contrast. Also, sometimes in more sensitive devices anti-reflection film could be made at interface by use of meta-materials (cylindrical or conical structures) to minimise reflection and maximise absorption [5].

- **CMOS compatible and cost effective**

  After successful simulations, realisations and optimizations of different parameters of device we have to fabricate our device for real time working by use of CMOS technology. So one should take care that material which is selected for making device could be easily fabricated at genuine cost, so that price of final product must be in reach of consumer.

Types of photoconductivity:

- Intrinsic photoconductors

  Absorption across primary band-gap, E_g , creates electron and hole photo-carriers.

- Extrinsic photoconductors

Absorption from (or to) impurity site in gap creates photo generated carriers in conduction or valence band.

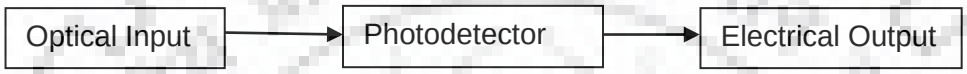

FIGURE 2: Basic Conversion System

Definition and Short introduction of terms associated with photodetectors that are used in this report:-

1. **Dark Current: I_D**

   Dark current is the bias current flowing in detector, when it is in total dark or no light is incident on it. It is kept as minimum as possible to increase sensitivity of detector, since it contributes to noise power of the detector output. Under working condition total current flowing through external circuit of photodetector is sum to mainly two currents i.e. dark current and photocurrent.

2. **Quantum efficiency: η**

   It is the ratio of no. of electron hole pairs generated in the active region which reaches the electrode without immediate recombination to no. of photons incident on active region of detector.

$$\eta = \frac{\text{No. of EHPs generated}}{\text{No. of Photons incedent}} = \frac{Pabsorbed}{Pincedent} \tag{2.2}$$

By using Beer lambert's law: $$p_{tr} = p_{in}.e^{-\alpha.w} \tag{2.3}$$

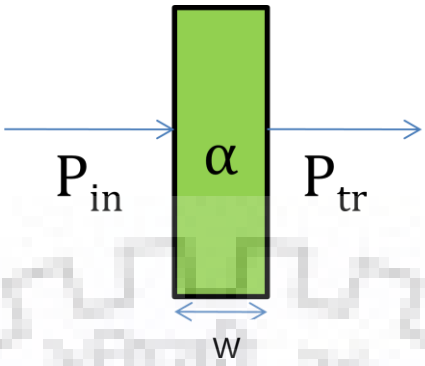

$$\eta = \frac{p_{ab}}{p_{in}} = \frac{p_{in} - p_{tr}}{p_{in}} = \frac{p_{in} - p_{in}.e^{-\alpha.w}}{p_{in}} = 1 - e^{-\alpha.w}$$

$$\eta = 1 - e^{-\alpha w} \quad (2.4)$$

3. Responsivity: R

Responsivity is defined as photocurrent produced per unit input power.

$$R = \frac{I_P}{Pin} \quad (2.5)$$

Also,

$$R = \eta \frac{\lambda(\mu m)}{1.24} G \quad (2.6)$$

Where,

η = Quantum efficiency.

λ = wavelength of incident photon in micrometers.

G= gain factor of device

4. Gain factor: G

Gain factor is a kind of amplification factor for very small electrical output of a photodetector. By taking care of following parameters, gain factor could be adjusted according to achieve large photocurrent for very small optical power input. But on cost of operating speed of detector i.e. in order to get large responsivity speed of operation of device gets reduced so ultimately bandwidth is reduced.

Photoconductor could be designed with large gain by controlling following two parameters are:

τ = excess carrier recombination lifetime.

t = carriers transit time.

$$G = \frac{\tau}{t} \tag{2.7}$$

$$\frac{1}{t} = \frac{1}{te} + \frac{1}{tp} \tag{2.8}$$

$$te = \frac{l}{\upsilon e} = \frac{l}{\mu e \times \varepsilon} \tag{2.9}$$

$$tp = \frac{l}{\upsilon p} = \frac{l}{\mu p \times \varepsilon} \tag{2.10}$$

5. Incident photon flux: φ

No. of photons incident per unit time on detector material is called as incident photon flux. It varies from source to source and also affected by distance between source and detector or due to variation of angular displacement.

$$\phi = \frac{P_{in}}{h\nu} \tag{2.11}$$

$$\phi = \frac{\text{energy incident} \,/\, \text{time}}{\text{energy of one photon}} \tag{2.12}$$

6. Photocurrent: I_p

Current flowing due to drift of excess carriers generated by incident photons under applied field. For photocurrent generation light falling on device active region must be of suitable wavelength. Under working condition (when device is biased and light is incident on it) total current flowing in external circuit is the sum of dark current and photocurrent.

$$I = I_D + I_P \tag{2.13}$$

Also,

$$I_P = R.P_{in}$$

So, here all the important parameters of a photodetector is explained and hence these concepts and relations can be used further in this report for discussions and interpretations [3, 4].

Applications:-

Photodetectors are used to build circuits dealing with:

- Optical Switches.
- Sensors.
- O to E convertors of oscilloscopes.
- Optical communication receivers.
- Various types of cameras.

2.1 PHOTOCONDUCTORS

The simplest form of photodetectors is photoconductors. This device is fabricated with a simple semiconductor material only along with two electrodes in direct contact with semiconductor material.

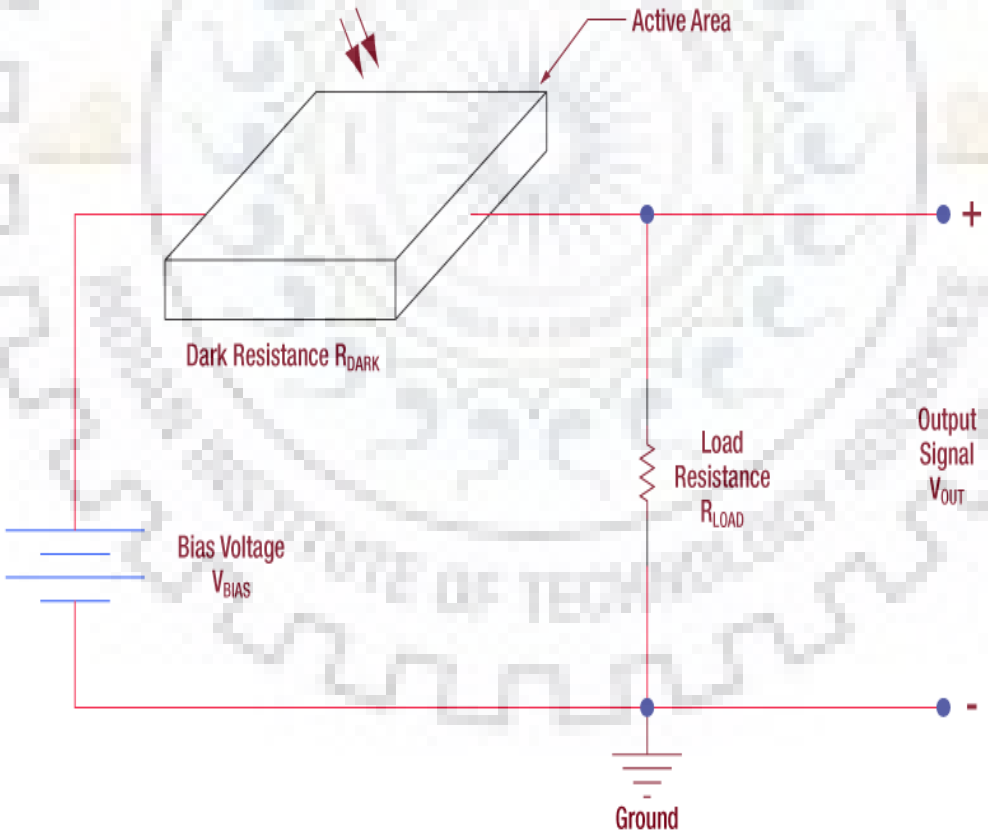

Figure 3 Basic Configuration of Photoconductor.

Here, the configuration shown in the figure is using voltage division rule to provide output voltage proportional to the incident light falling on the active area.

$$. V_{OUT} = \frac{R_{LOAD}}{R_{LOAD}+R_{DARK.}} . V_{BIAS} \quad (2.14)$$

V_{OUT} is proportional to the light falling on the active region of detector and simultaneously it is designed in such a way that the gain factor G discussed above is very large which results in large value of responsivity but on the cost of working speed and bandwidth of device. This trade-off could be explained with reference to the fact that gain bandwidth product of the device remains constant.

$$GAIN * BANDWIDTH = CONSTANT \quad (2.15)$$

If one increases then the other one has to decrease. Under dark conditions the current flowing in the circuit is very less and it contributed to the noise power of the device. When light falls on the device, current increase in very large proportion due to addition of photocurrent to the dark current. When current flow through circuit increases, potential drop across R_{LOAD} also increases which could be easily detected or measured by instruments.

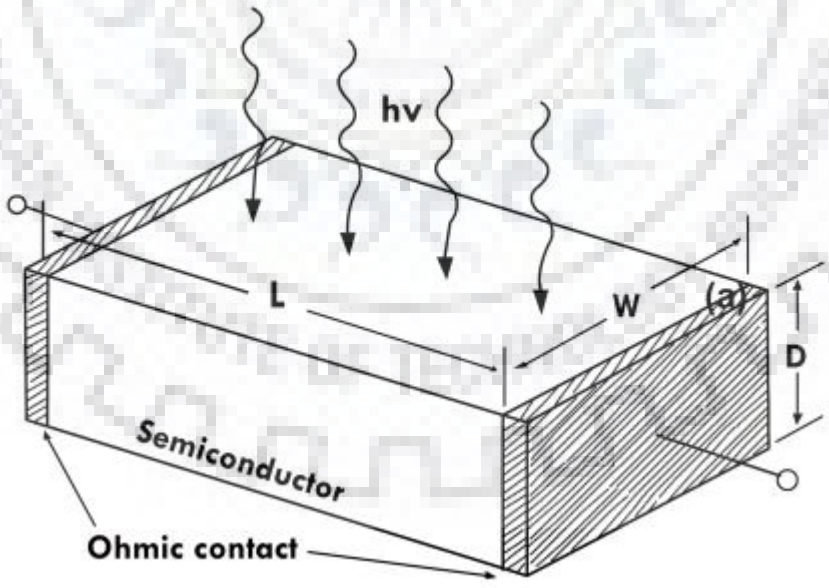

Figure 4: Device structure of photoconductor [3].

2.2.1 MSM detector

A metal–semiconductor–metal photodetector (MSM detector) is a photodetector device containing two Schottky contacts, i.e., two metallic electrodes on a semiconductor material. During operation, some electric potential is applied to the electrodes. When light falls on the semiconductor placed between the electrodes, it generates electron hole pairs, which are swept by the electric field and give rise to photocurrent.

In practical applications one normally uses some kind of interdigitated electrode structure (finger like structure), where the finger spacing can be as small as 1 μm. The electrode structure can also be ring - shaped, covering an approximately circular area. For high quantum efficiency transparent electrodes with anti-reflection films are used. For high speed, travelling-wave configurations are used, where the input light is sent through an optical waveguide containing the absorbing layer. The electrodes are deposited on top of the waveguide, giving rise to a coplanar waveguide line for the generated microwave signal.

MSM detectors can be made faster than photodiodes. Their detection bandwidths can reach hundreds of gigahertz (with an impulse response function narrower than 1 ps), making them suitable for very high-speed optical fibre communications. A practically important aspect of MSM photodetectors, is that they have relatively simple planar structure that are particularly suitable for monolithic integration with other components on optoelectronic circuits [6].

2.2.2 Photodiodes

A photodiode is based on simple p-n junction or p-i-n junction and avalanche photodiode.. In p-n junction diode carriers are generated in depletion region, by applying large reverse field carriers are swept toward electrodes giving rise to photocurrent. Disadvantage of p-n junction is that the depletion width is small and depends on the doping concentration of the p and n side. It is not possible to design depletion region of large length, so active region will be small. This problem can be solved by using p-i-n photodiode in which long intrinsic region or lightly doped n-type region. Here carriers are produced in large intrinsic region and are swept by reverse field. Electrons that are generated move to n side and holes towards p side. Advantage of p-i-n diode is that quantum efficiency, sensitivity and gain can be controlled by thickness of intrinsic region of the device whereas p and n side remains fixed.

Whereas, avalanche photodiode is very sensitive diode due to avalanche multiplication process working in it. When photon is incident on active region it generates free electron hole pairs, these electron hole

pairs when accelerated under large voltage they collide with the lattice, and generates further one more electron hole pairs, this process repeats again and again giving huge gain and high sensitivity. They are used in applications where gain is major parameter of concern. Compared to normal diodes avalanche diode works at more reverse bias voltage as more energy is required for starting of avalanche multiplication process. Avalanche diode requires large negative voltage for working, for silicon diode it is typically between 100-200 volts. With this applied voltage they see a current gain of around 100.

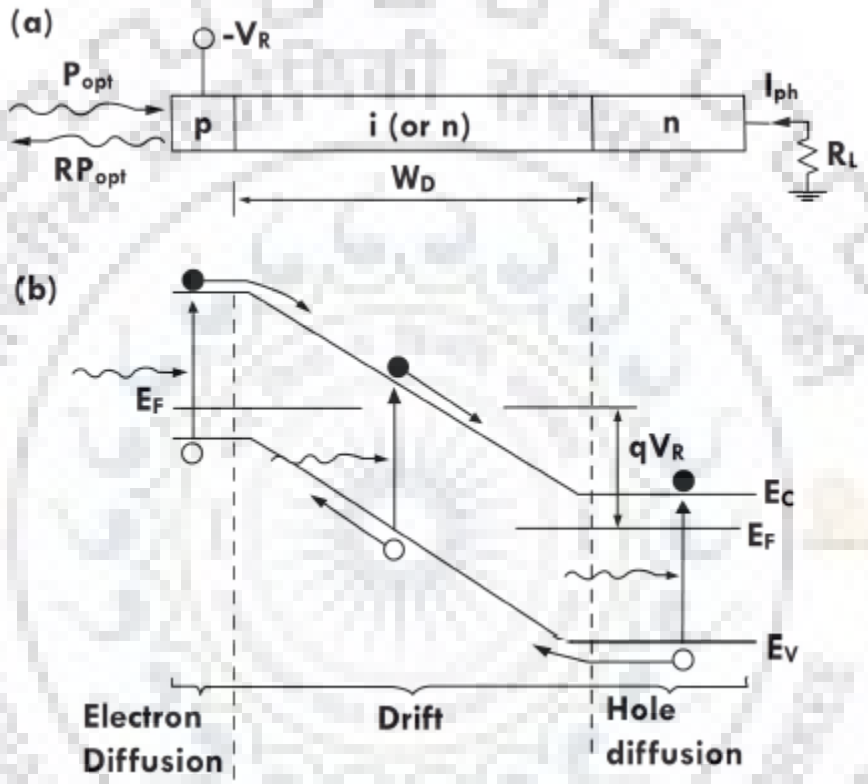

Figure 5 P-i-n Diode [3]

(a) p-i-n diode device with thin p and n side and wide intrinsic region.

(b) Energy band diagram showing movement of electron & holes under influence of applied bias.

Let α be the absorption coefficient in intrinsic region and it is wavelength specific. Let W_D be width of intrinsic region. For high quantum efficiency product of $\alpha.W_D >> 1$.The trade-off is that the device length is longer and this increases carriers transit time and hence the response time [4].

2.2.3. Phototransistor

Phototransistor effectively converts light into electrical signal. Unlike normal transistor where base current is controlled by voltage source here base current is produced and controlled by incident light. A

common type of phototransistor, called a photo-bipolar transistor, is in essence a bipolar transistor encased in a transparent case so that light can reach the base–collector junction. The electrons that are generated by photons in the base–collector junction are injected into the base region, and this photodiode current is amplified by the transistor's current gain β (or h_{fe}). If the base and collector leads are used in working and the emitter is left unconnected, the phototransistor becomes a photodiode. Phototransistors also have significantly longer response times, compared to photodiodes.

2.2.4 Waveguide photodetectors

In the preceding sections photodetectors discussed are vertically illuminated. In vertically illuminated photodetectors (VIPD), the optical signal propagates in direction perpendicular to the junction interface of device. This situation leads to a trade-off between the carrier transit time and the quantum efficiency, resulting in a limitation on the bandwidth-efficiency product of the device. Another limitation of a high speed VIPD arises from trade-off between the bandwidth and saturation power. A large bandwidth for a VIPD requires a small absorption volume, which results in a high carrier concentration at a given power level of optical signal. The space charge effect in the active region caused by high carrier concentration sets a limit on the saturation power of photodetectors. Waveguide photodetectors or guided-wave photodetectors are developed to overcome these limitations. Most of the photodetectors such as MSM photodetectors, p-i-n photodetectors and avalanche photodiode can be in guided-wave device form. In a guided wave photodetector, guided optical signal propagates in a direction that is parallel to the junction interfaces and is perpendicular to the drift of the photo-generated carriers. Using the technique waveguide photodetector of responsivity ~ 48A/W is made for working wavelength of 1550nm.[7] The major advantage of a guided-wave photodetector over a VIPD is that it's carrier transit time can be independently reduced without sacrificing it's quantum efficiency and saturation power.

2.3 Silicon waveguides

SOI waveguides channels the light through a transverse and lateral confinements in silicon core (n=3.47) which is surrounded by its oxide as bottom cladding (n=1.44) and low index top cladding. Generally, silicon waveguides are fabricated using electron-beam also by reactive ion etching, on CMOS manufacturing tools. To follow single-mode condition (at 1550nm communication wavelength) the cross section dimensions need to be in sub-micrometer range, with increasing widths for decreasing thicknesses. Cross sections may vary from a wide, thin 600x100 nm to a square 300x300 nm. The

commonly used dimensions for the waveguides are 400 nm to 500 nm for width, and 200 nm to 250 nm for height. In this thesis we have used waveguide dimension as 400x800 nm. The refractive index contrast between core and cladding is very high, which gives rise to very strong confinement that enables light guiding in bends with very small radii without radiation losses. At the core/cladding interface, the normal component of displacement D = ε*E must be continuous. Therefore, the field amplitude at the cladding side of the interface will be stronger for a mode with the dominant E-field polarized normal to the interface. If the waveguide width is larger than its height (the most commonly used geometry), the ground mode will have a quasi T E polarization, with a strong discontinuity on the sidewall surface. Likewise, the TM mode will have a discontinuity on the top and bottom surface.

Propagation losses in silicon wires originate from multiple sources, and recent advances in process technology (in various groups) have brought the losses down to 2–3dB /cm with air cladding and less than 2dB/cm with oxide cladding.[1] This difference can be explained by looking at different loss contributions. A lot of effort is put into the optimization of fabrication processes to minimize the surface roughness. The losses are correlated with the periodicity of the roughness as well as its dimensions, and scale dramatically with the index contrast.

Here is a comparison of different cross section area dimensions

- 400 nm X 800 nm

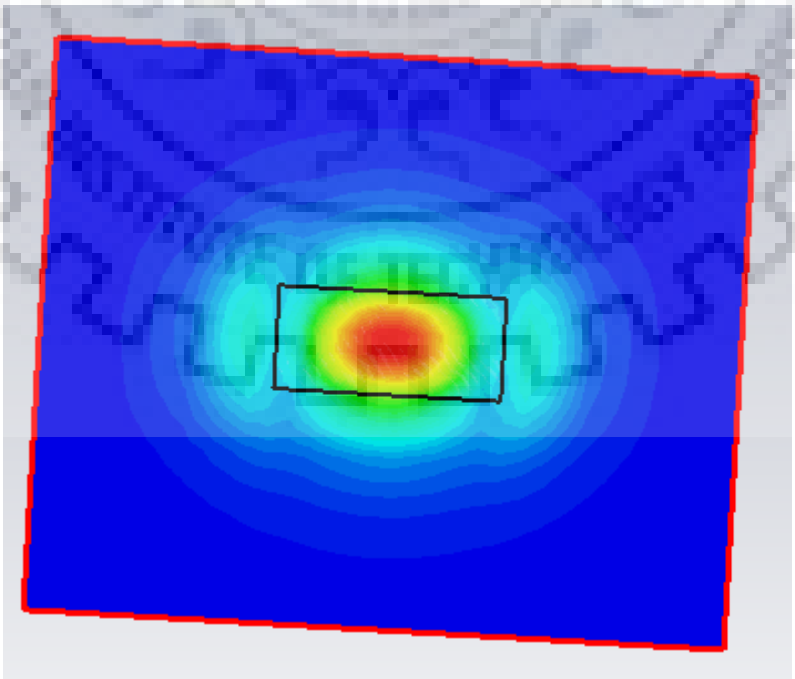

- 250 nm X 450 nm

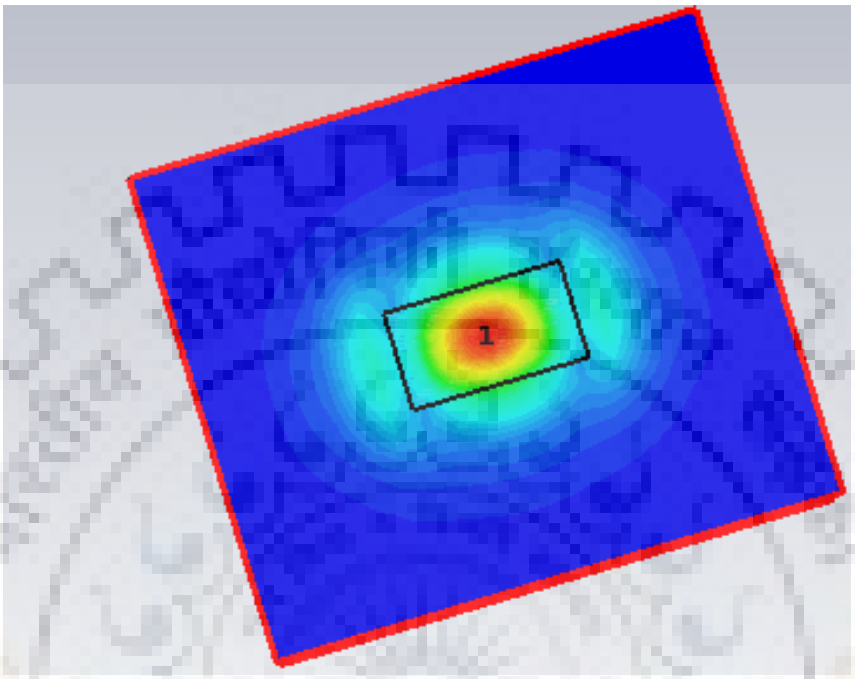

- 250 nm X 500 nm

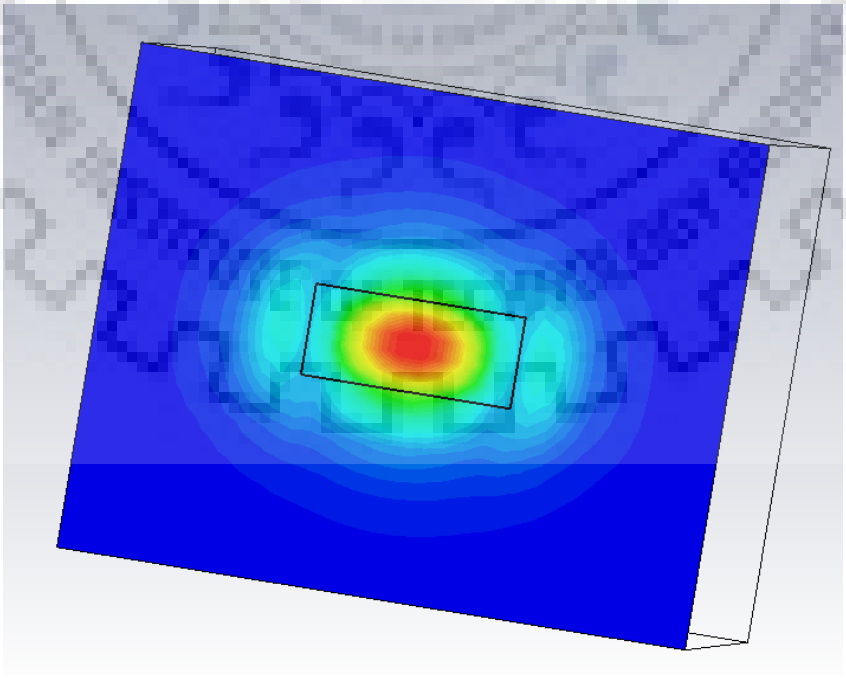

- 300 nm X 300 nm

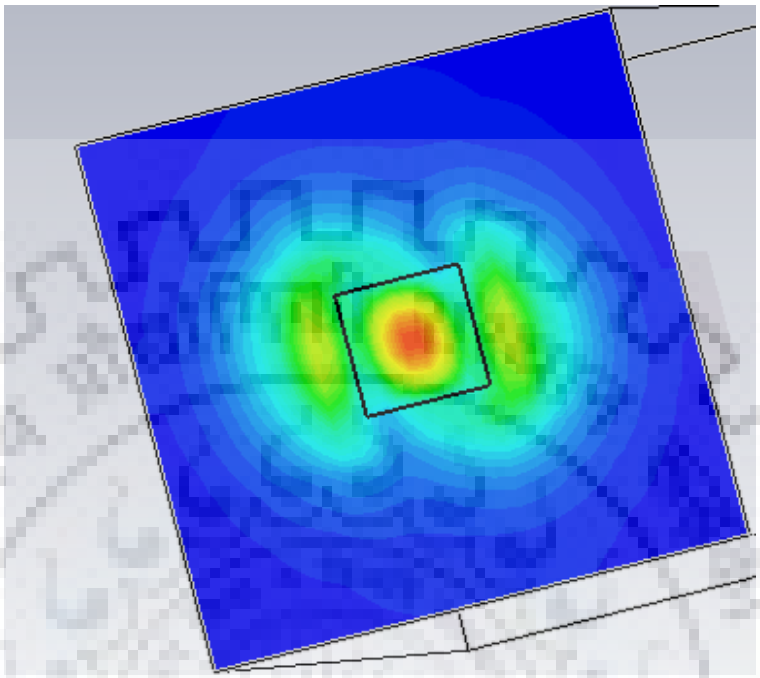

2.4 Structure for simulation

In the simulation software CST microwave studio a waveguide is modelled on silicon dioxide substrate and $Ge_2Sb_2Te_5$ is placed inside the waveguide and it is working as active region of detector.

- Model in CST microwave studio

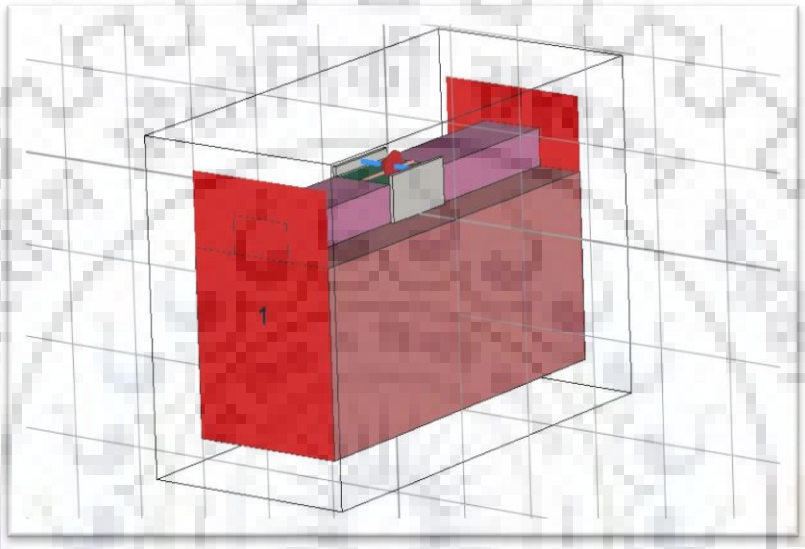

- Propogation of mode in waveguide (cross sectional view)

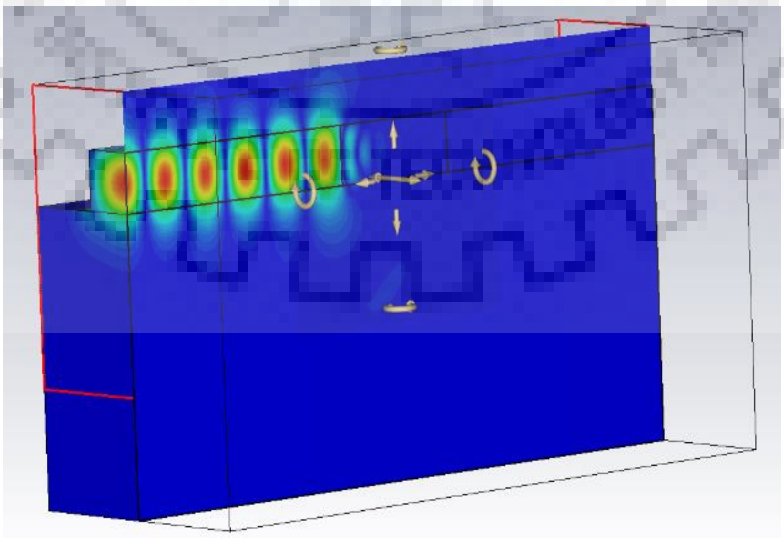

Unit 3: Phase Change Material

3.1 Introduction:-

What is phase change material?

Phase change materials (PCMs) are those materials that change phase from one phase to other phase at a particular temperature. The phases can be two or more than two and the material can be switched among these phases. A large amount of heat is required to melt PCMs and large amount of heat is released when it freezes.

The different phases have different physical properties such as thermal conductivity, electrical resistivity etc. There is a large resistance contrast between the amorphous and crystalline phases of PCMs. The amorphous phase is highly electrically resistive, while the crystalline phase exhibits low electrical resistivity.

Examples of PCMs are $Ge_2Sb_2Te_5$, Sb_2Te and In doped Sb_2Te etc.

Scalability of phase change materials

Since 1960s, the idea of applying phase change materials to electronic memory got its way. But the interest in PCM technology was triggered after the discovery of fast (<100 ns) crystallizing materials such as $Ge_2Sb_2Te_5$.The physical properties of nanoscale materials is different from those of bulk materials and is a function of size. The ratio of surface atoms to volume atoms is greater in nanoscale matter than that in bulk matter. Therefore, the nanoparticles have a lower melting point. The parameters of phase change materials are of great importance for PCM applications. The optical properties are also function of film thickness. Crystallization temperature is one of the most important parameters of PCMs. It is the temperature at which crystallization is fast. It varies as a function of material composition and thickness of film. Melting temperature is another parameter that varies with material composition and thickness of film. For very thin films, reduction in melting temperature has been observed. This is beneficial for device applications because lower melting temperature needs less power. The thermal conductivity of PCMs reflects the thermal response of a PCM device to an optical/electrical

pulse. So it is also an important parameter. The materials which have been studied so far (GST-225, Sb_2Te, Ag and In doped Sb_2Te), however, show only a slight variation in thermal conductivity values (between 0.14 and 0.17 W/mK for as deposited amorphous state and between 0.25 and 2.47 W/mK for crystalline state). In conclusion, it has been observed experimentally that :

- The crystallization temperature increases as the dimensions are reduced.
- The melting point is reduced as the dimensions are reduced.
- The resistivity increases as the dimensions are reduced.
- The thermal conductivity reduces slowly with the reduction in film thickness.

3.2: Lattice structure of $Ge_2Sb_2Te_5$

$Ge_2Sb_2Te_5$ (GST- 225 or GST) is a compound of germanium, antimony and tellurium. It is a phase change material from the family of chalcogenide glasses. GST is found in two states- crystalline and amorphous. The crystalline phase has rock-salt structure. The Ge and Sb atoms occupy Na sites while the Te atoms occupy the Cl sites. GST is used in electrical phase change memory, Rewritable optical discs and DVDs etc. [8].

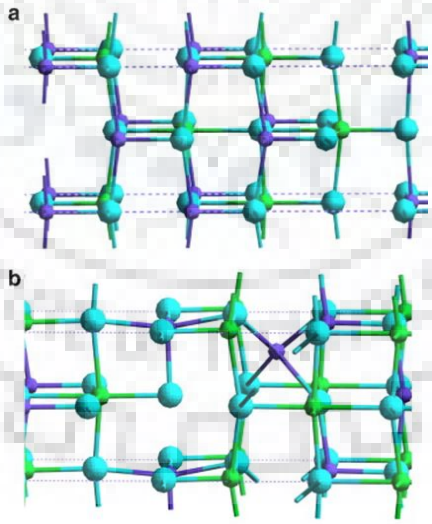

Fig 6 (a) Relaxed rock–salt-like structure of crystalline phase of $Ge_2Sb_2Te_5$.
(b) Relaxed structure of glassy phase of $Ge_2Sb_2Te_5$ [8]

3.3: Electrical properties of $Ge_2Sb_2Te_5$

Being used as active material in photodetector, electrical properties of GST is very important to be known. Energy band gap of a-GST is around 0.7 eV and that of c-GST is 0.5 eV and the wavelength of light that could be absorbed by these phases are 1550nm and 2400 nm respectively. Variation of electrical conductivity with temperature of a typical 80 nm thick film of a-GST is shown in following plot:

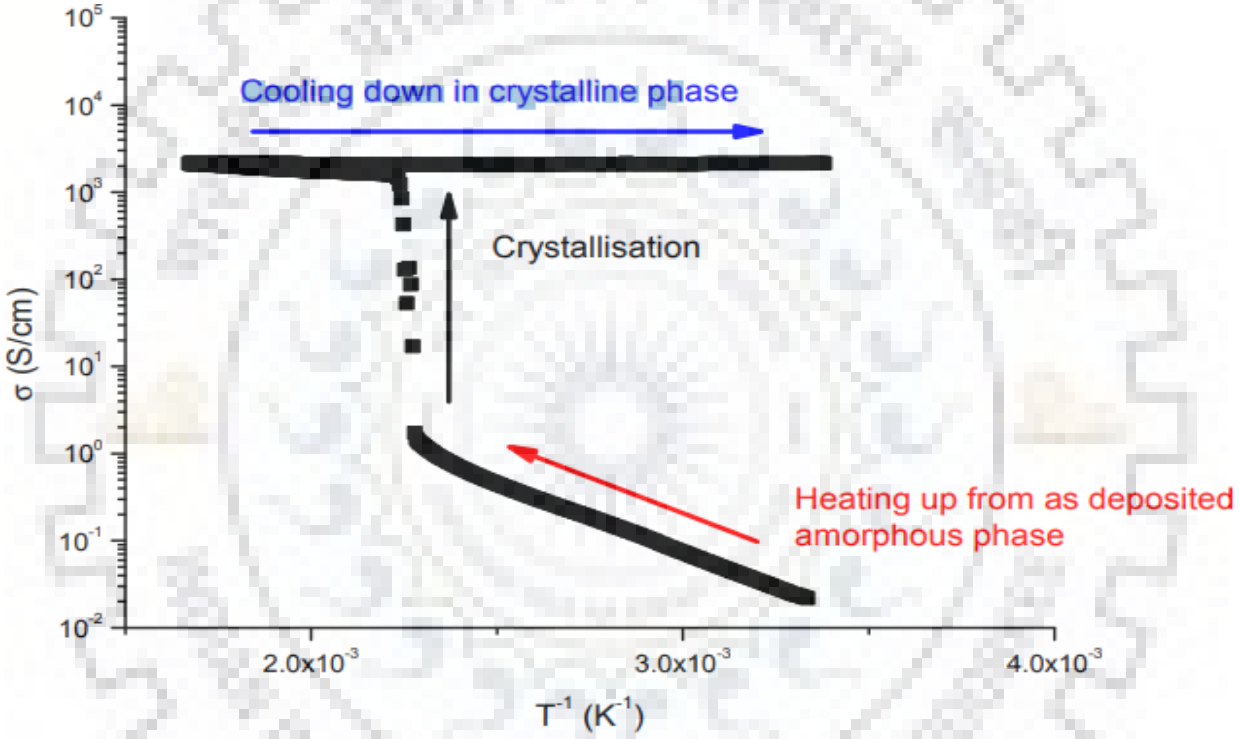

Fig. 7 Variation of conductivity with temperature [11]

Above plot between σ and T^{-1} reveals a thermally activated characteristic of a-GST upon heating which is represented by straight line (red arrow). The activation energy for transportation typically ranges from 0.3-0.5 eV, having a value half the optical band gap. At a temperature of 170° C this film crystallises accompanied by large step-like increase in conductivity. Upon further heating and subsequent cooling the film remain in temperature independent metallic-like state. Values of room temperature conductivity usually ranges from 10^{-5} - 10^{1} S/cm and from 10^{0} - 10^{4} S/cm for amorphous and crystalline PCMs respectively.[9,10]

Process for change of phase:

Conversion	Condition
1. a-GST to c-GST	Long duration current pulse is applied of low amplitude.
2. c-GST to a-GST	Short duration large amplitude current pulse is applied.

Table 1 Process of phase change

Resistance of PCMs:

Amorphous	High resistance	Reset	0
Crystalline	Low resistance	Set	1

Table 2 Resistance with states

- Amorphous phase of PCMs have high resistance and can be considered as reset state or '0' state.
- Crystalline phase of PCMs have low resistance and can be considered as set state or '1' state.

Unit 4: Simulation Software

CST studio suite is one of the effective idea implementation platform for a wide range of electromagnetic field issues and related applications. The program gives us an easy to understand interface for dealing with plethora of ventures and perspectives.

The CST STUDIO Suite software package provides the following simulation modules;

- **CST MICROWAVE STUDIO**
- CST EM STUDIO
- CST PARTICLE STUDIO
- CST DESIGN STUDIO
- CST PCB STUDIO
- CST CABLE STUDIO
- **CST MPHYSICS STUDIO**

Structure Modelling: -

CST MICROWAVE STUDIO, CST EM STUDIO, CST PARTICLE STUDIO, CST MPHYSICS STUDIO share a typical structure simulating tool. The primary reason for this part is to give an outline of the structure modeller's numerous abilities.

Postprocessing: -

Once a simulation is completed, result information will appear in the navigation tree. CST STUDIO SUITE contains good postprocessing abilities which incorporate different alternatives for visualising the outcomes and computing auxiliary amounts. It would be ideal if you refer to module particular documentation and the online help framework for more data.

Result Navigator window:

The result window offers a processed data plots to visualise the quantity of showed results and wanted parameter ranges or plot where 0D comes about. Changing the choice in the route tree enables you to review different outcomes process of the dynamic parameter mix determination.

The parametric plotting functionality allows for convenient access of typical parametric results without the need for further setting up more advanced postprocessing operations. The automatically stored parametric results can also be used directly for optimization of device. Please refer to the online documentation for more information which every user is provided with.

The solvers included in CST EMC STUDIO have been selected to allow a wide range of EMC workflow to be carried out in a straight forward way.

- The transmission line matrix (TLM) solver is time domain method which is especially well suited to EMC simulation. The TLM solver can use octree gridding to significantly reduce simulation time on extremely complex structures, and also supports analytic compact model representations of fine details.
- The transient solver, based on the finite integration technique (FIT), is a general purpose time domain solver and is best suited to broadband simulations of radiated emissions and susceptibility.

- The frequency domain solver is based on the finite element method (FEM), and is often used to simulate conducted emissions. The frequency domain solver includes a special meshing engine optimized for PCBs, which allows various complex boards to be simulated faster than conventional methods.
- The cable harness solver is a specialized solver for simulating cables in complex environments. There is a bidirectional coupling present between the cable harness solver and the time domain solvers, allowing cable harnesses to be integrated into a 3D model and analyzed using bidirectional simulation.

CST MICROWAVE STUDIO (CST MWS) is a specialist tool for the 3D EM simulation of high frequency components. CST MWS' unparalleled performance makes it the most trusted choice in leading R&D departments all over the world.

CST MWS enables the fast and accurate analysis of high frequency operating devices such as antennas, filters, couplers, planar and multi-layer structures and SI and EMC effects. Exceptionally user friendly, CST MWS quickly gives you an overview of EM behavior of your high frequency designs.

CST promotes Complete Technology for 3D EM. Users of our software are given great flexibility in tackling a wide application range through the variety of available solver technologies. Besides the flagship module, the broadly applicable Time Domain solver and the Frequency Domain solver, CST MWS offers further solver modules for specific applications. Filters for the import of specific CAD files and the extraction of SPICE parameters enhance design possibilities and save time. In addition, CST MWS can be embedded in various industry standard workflows through the CST STUDIO SUITE® user interface.

Post-processing Formats: -

The post-processing Formats take into account adaptable handling of 2D/3D Fields, 1D Signs, or scalar qualities. All characterized post processing Layouts are assessed after each count amid parametric scopes and enhancements. The ascertained information is then put away parametrically to take into account adaptable access to the whole informational collection [12].

Unit 5: Methodology

To start with the waveguide photodetector structure I considered following steps as mentioned chronologically. To construct photodetector I started with simulation of straight waveguide of 400nm X 800nm dimensions with a set of few other dimension changes relating to cross section area and the length of the waveguide. The waveguide was constructed by taking silicon dioxide as substrate. This was followed by learning of the method of placing waveguide ports at the terminals of waveguide and launching light in it. While light is being propagating in waveguide one can easily monitor the TE and TM modes at the ports and also at any point inside waveguide. Next step was introduction of GST material its two states a little background reading, with the guide's insight I assumed GST physical dimensions and obtaining standard optical and electrical properties. GST block's position and physical dimensions were altered in specific range and result was monitored.

Size of GST block placed in waveguide is optimized for maximum absorption by application of length sweep in CST studio. Absorption coefficient of GST is calculated with the help of different parametric equations and comparison with different journals is done. Further paper reading and insights from research scholars, I made electrodes across the GST and applied bias voltage to it through discrete port. By making use of local coordinate system u, v & w a current monitor loop is designed that is across the whole cross section of GST. This current monitor loop is able to measure current flowing through GST between electrodes.

In the beginning, when simulations were done without electrodes and applied bias voltage the parameters of photodetectors were theoretically calculated and plotted with the help of MATLAB. At that time only power input and power output was available for interpretation. At the parametric equations were transformed in form of P_{out} and P_{in} and theoretical results were plotted. Further, when current monitors were placed and discrete port was applied then we get directly the value of current flowing in the device. During simulations parameters like input power, frequency or wavelength of light, magnitude of biasing voltage is being changed and change in current is observed.

After performing all the simulations result plotting and observation and analysis was performed. Every time while performing simulations, optical power to be used in simulation is given in setup solver. Setup solver does not take value of optical power directly but takes value of amplitude. Amplitudes corresponding to different optical powers are calculated by the relation:

$$P = \frac{A^2}{2} \tag{5.1}$$

During simulation we make use of wide range of frequencies of optical input applied. Values of different frequency dependent parameters such at different frequencies are also provided to simulation software before starting. Parameters like n, k, ε and ε' for different frequencies are provided at different stages of simulations. The Maxwell model allows one to relate ε and ε' to the refractive index n(ω) and extinction coefficient k(ω) [13]. The data in following table are acting as only set of few points but CST is able to fit these date points to continuous values of parameters. Data used here are shown in appendix.

Work done	Results
1. Theoretical calculation of different parameters of detector by taking certain assumptions.	Plots that are made in MATLAB are as follows: • η Vs λ (figure 9) • α Vs λ (figure 11) • R Vs λ (figure 10) • I_p Vs λ (figure 12)
2. Bias voltage is applied through discrete port placed between the two electrodes and current monitor is used to measure current.	• Here c-GST and a-GST are placed inside waveguide and current observed under different incident optical powers. • Then, for some fixed incident optical power bias voltage is varied and current is monitored. • Large range of variation in incident optical power is done keeping bias voltage fixed to get an idea of the threshold value of power that can be measured.

Table 3 Tasks performed

Unit 6: Results

6.1 Results under this section are theoretically calculated for c-GST used in simulation of photodetector:

- **Straight Waveguide (400 nm) x (800 nm) x (5 um)**
- **c-GST dimensions (400 nm) x (800 nm) x (1 um)**
- **bias voltage = 2V**

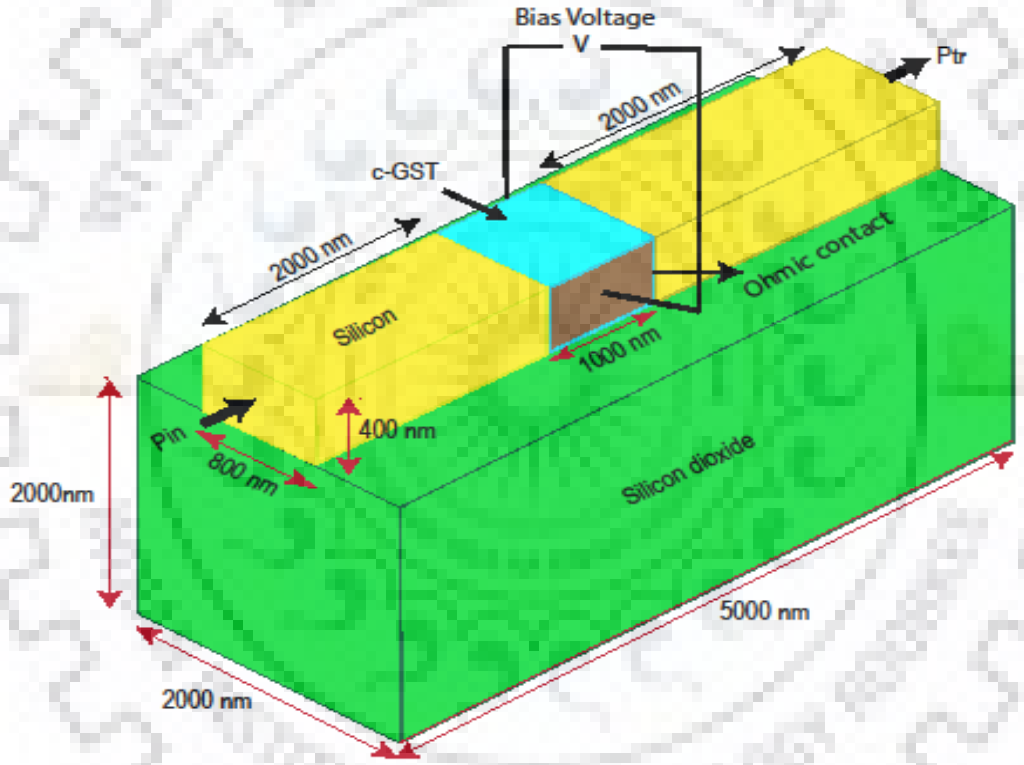

Figure 8 Schematic diagram of detector

By using formula of different parameters of photoconductor calculations are done. Few points are shown in following table:

λ(nm)	P_{in}(W)	η	Φ(sec^{-1})	Δ n	G=τ/t	R(A/W)	I_p(mA)
2400	0.005	0.85	$6.03x10^{16}$	$5.13x10^{16}$	30.423	50.06	250
2200	0.005	0.82	$5.53x10^{16}$	$4.53x10^{16}$	30.423	44.27	221
2000	0.005	0.78	$5.03x10^{16}$	$3.92x10^{16}$	30.423	37.74	188

Table 4 Calculated parameters

One can get a clear idea of photocurrent I_p calculated at 0.005W. For complete information following graphs are plotted in MATLAB:

- **Variation of Quantum efficiency (η) with Wavelength (λ)**

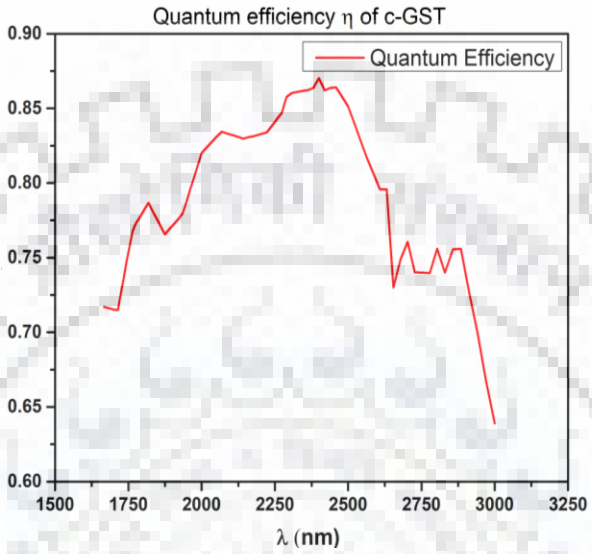

Figure 9 η Vs λ Plot

- **Variation of Responsivity (R) with Wavelength (λ)**

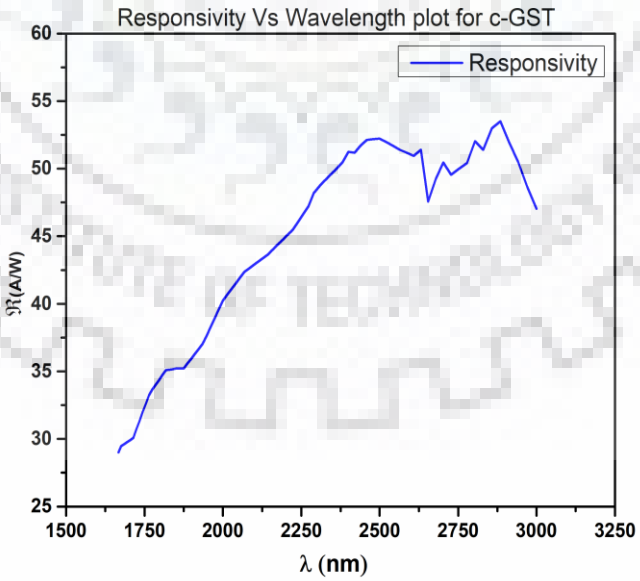

Figure 10 R Vs λ Plot

- **Variation of Absorption coefficient (α) with Wavelength (λ)**

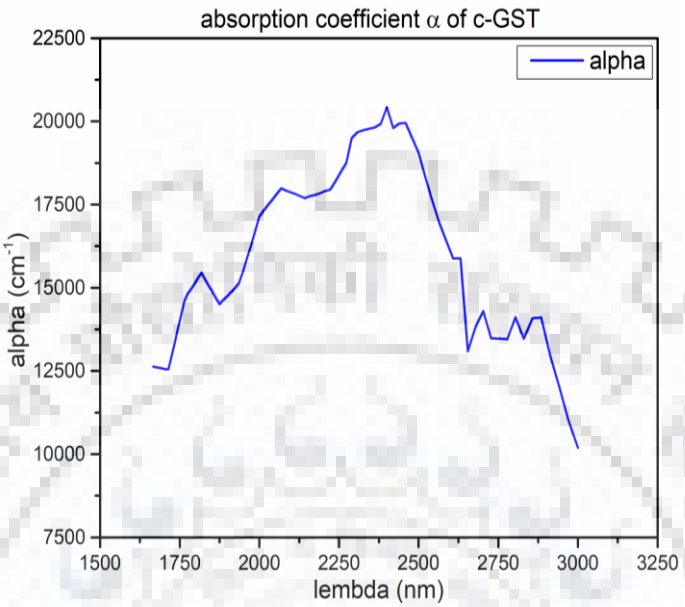

Figure 11 α Vs λ Plot

- **Variation of Photocurrent (I_p) with Wavelength (λ)**

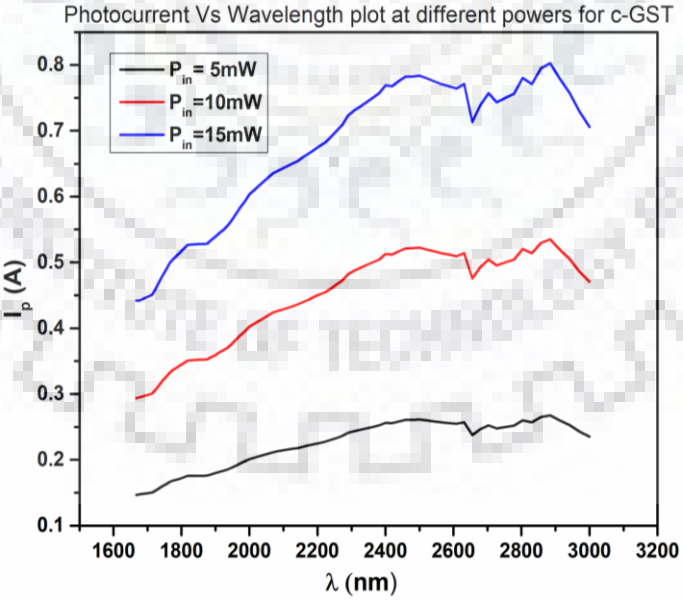

Figure 12 I_p Vs λ Plot

6.2 Results under this section are completely simulation based for both the phase a-GST & c-GST used in simulation of photodetector:

6.2.1 a-GST under different optical powers

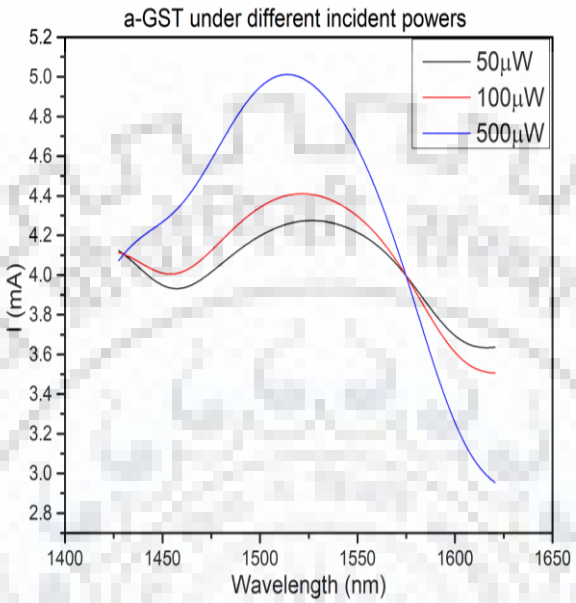

Figure 13 a-GST

6.2.2 c-GST under different optical powers

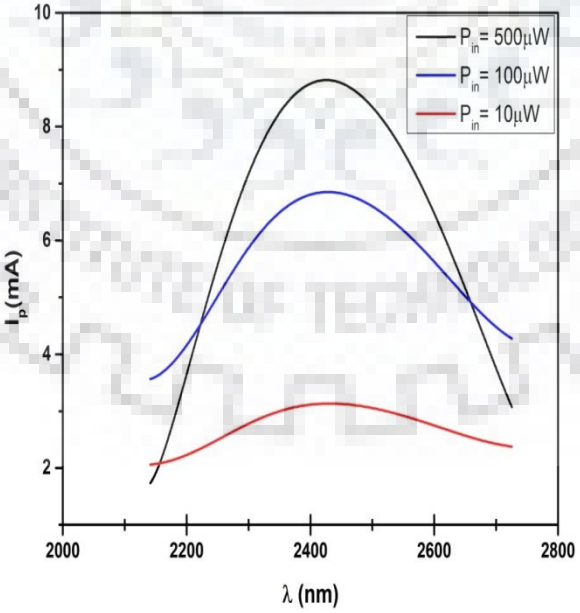

Figure 14 c-GST

6.2.3 a-GST under different bias voltages around 1550nm and 2200nm

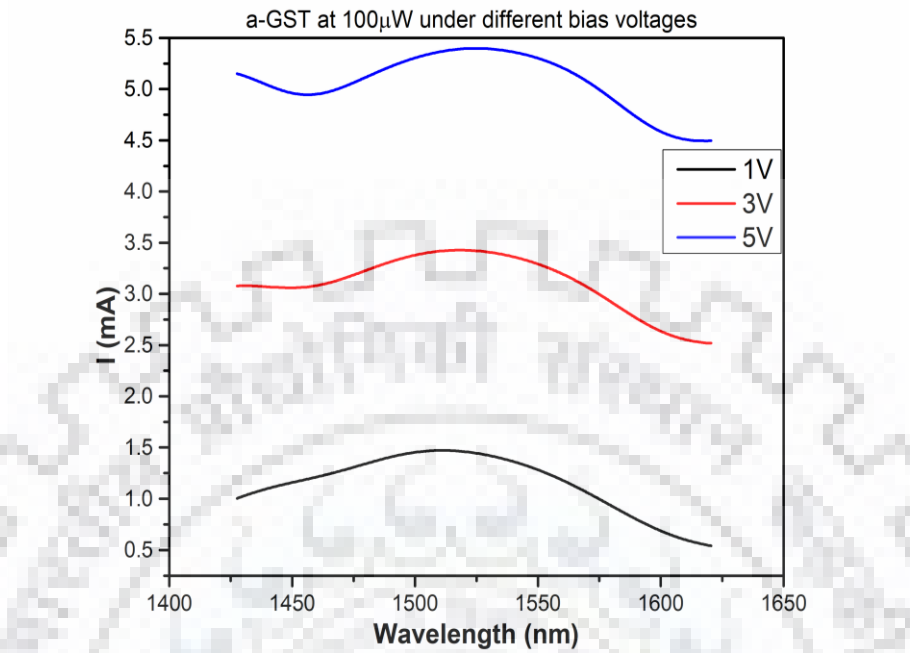

Figure 15 a-GST biased 1550nm

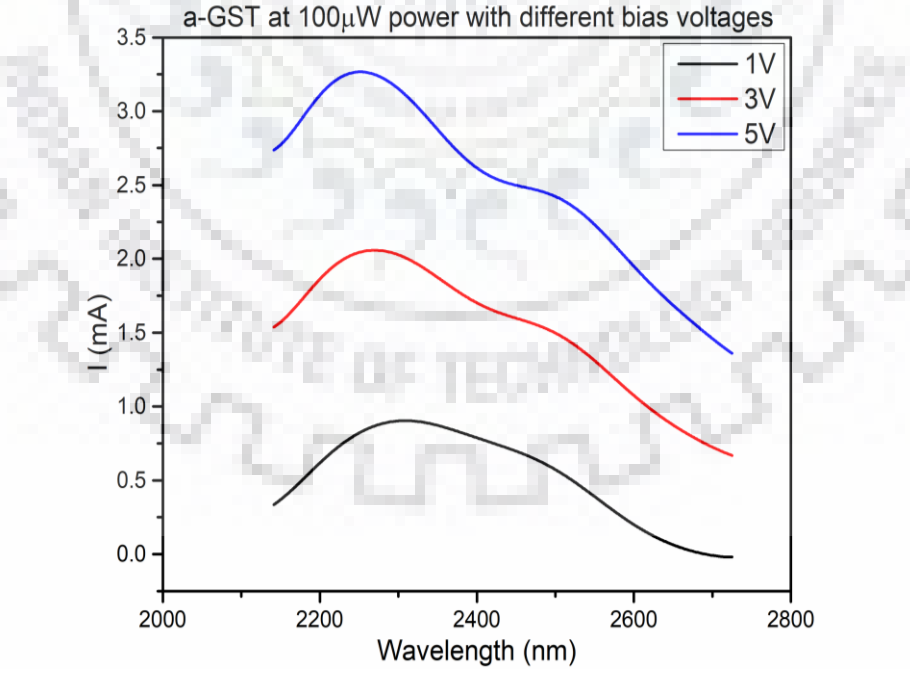

Figure 16 a-GST biased 2200nm

6.2.4 c-GST under different bias voltages around 1550nm and 2200 nm

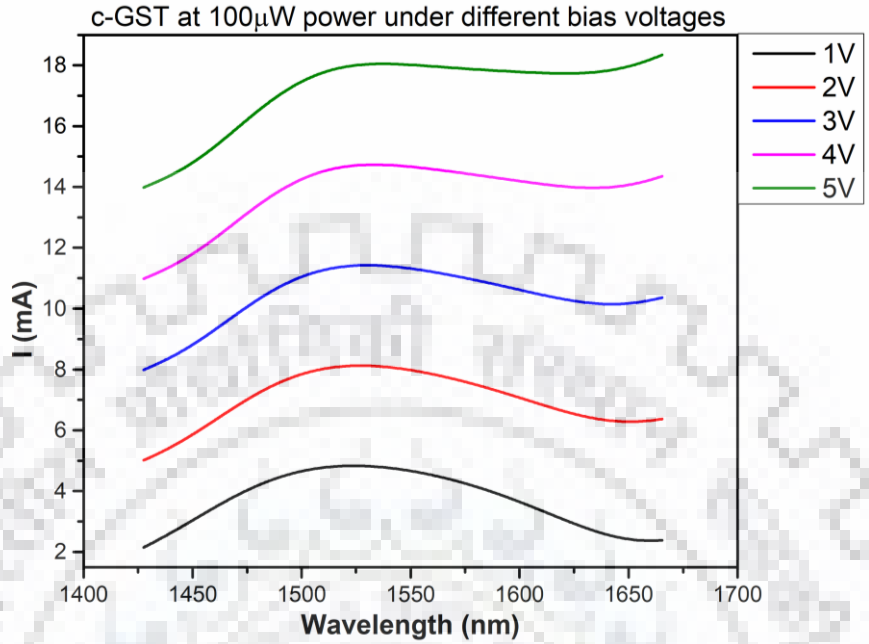

Figure 17 c-GST biased 1550nm

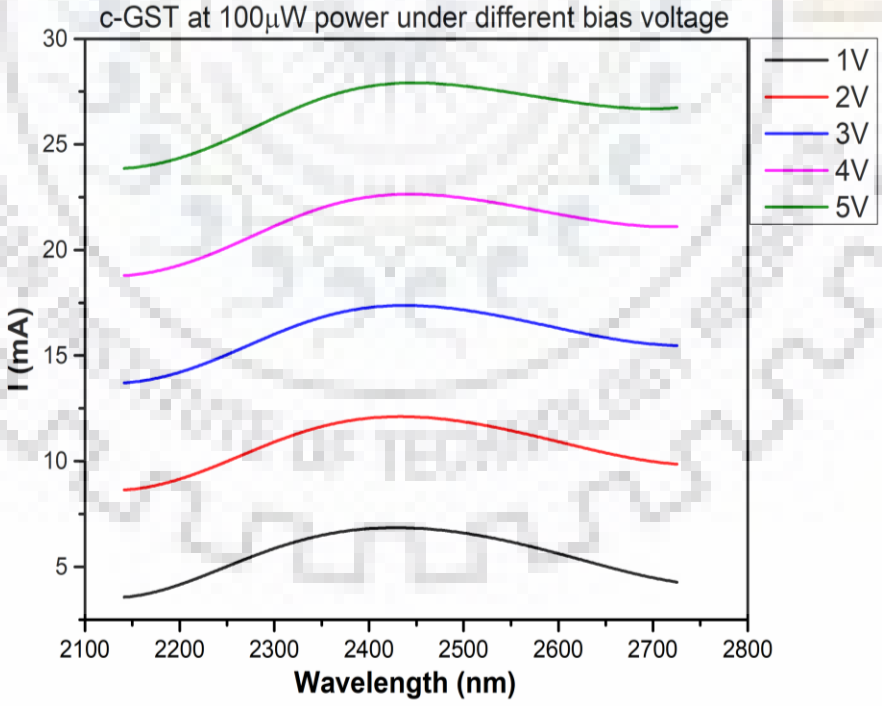

Figure 18 c-GST bias 2200nm

6.3 Large range of variation in incident optical power

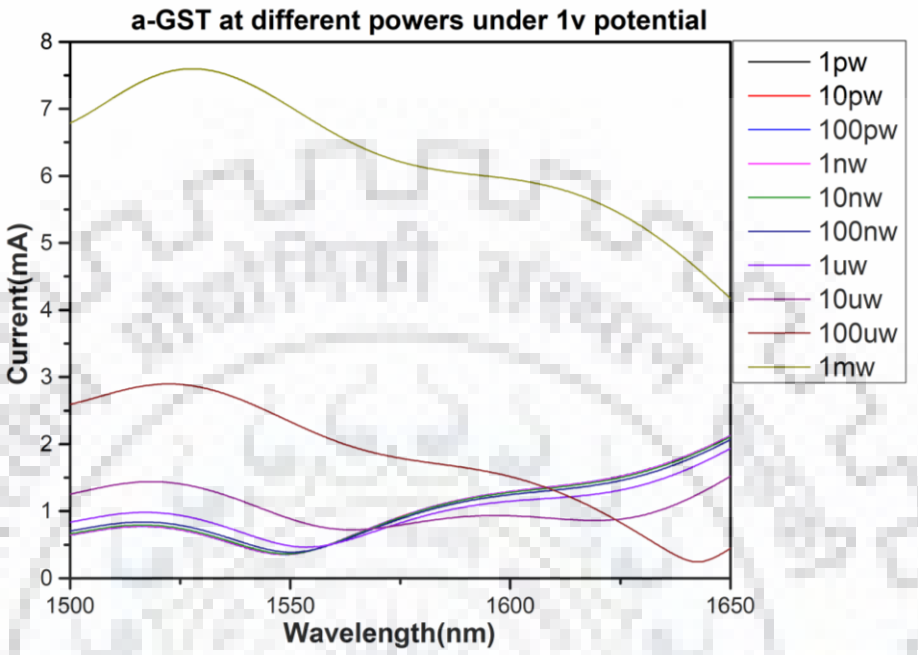

Figure 19 current 1

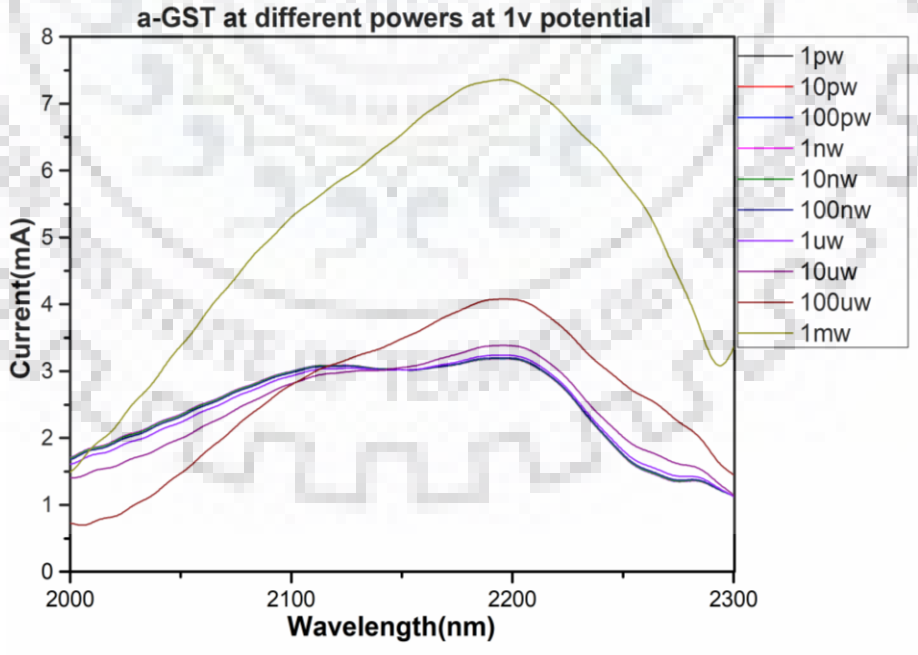

Figure 20 current 2

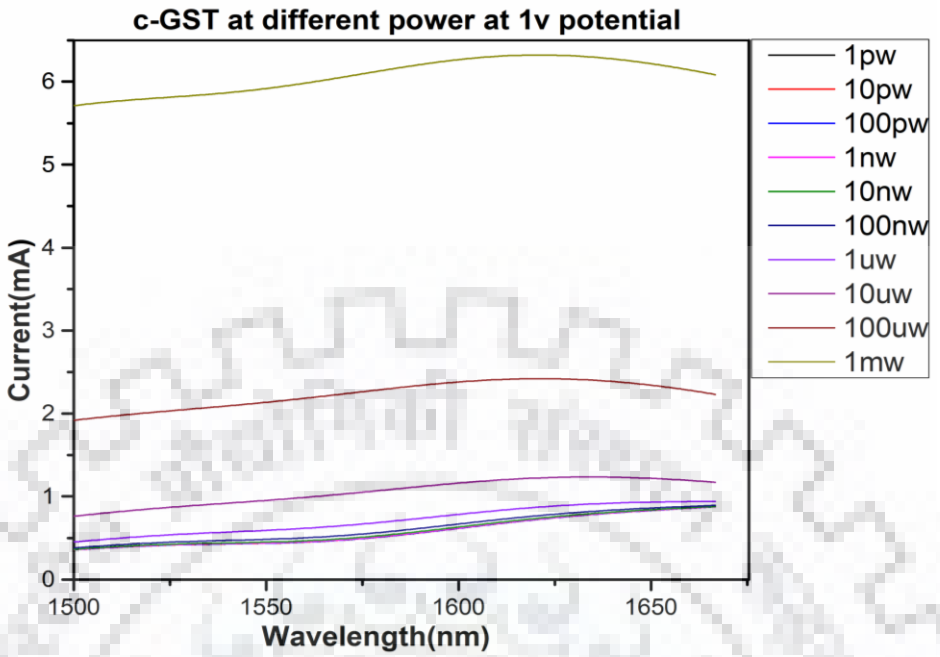

Figure 21 current 3

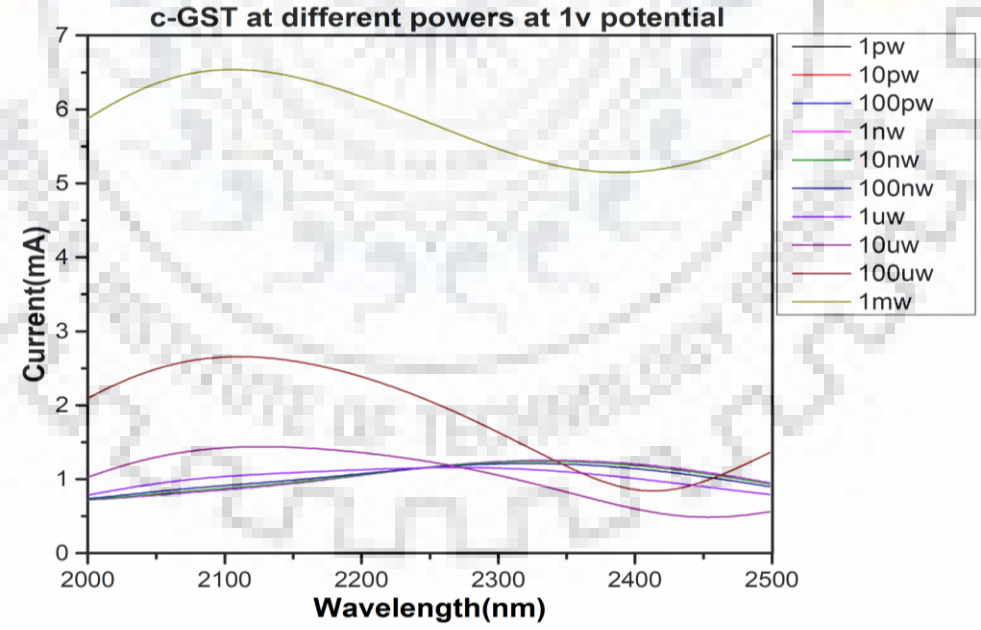

Figure 22 current 4

6.4 Analysis of Dark Current

In this section optical excitations from both the ports i.e. port 1 and port 2 are kept off and only discrete port is made to bias the PCM by 1V. Current monitored in this condition is termed here as dark current. Further, optical and electrical excitation is applied simultaneously with help of simultaneous option in setup solver window of CST. Current monitored under this condition is termed as total current. According to eq.2.13 difference between total current and dark current is termed as photocurrent.

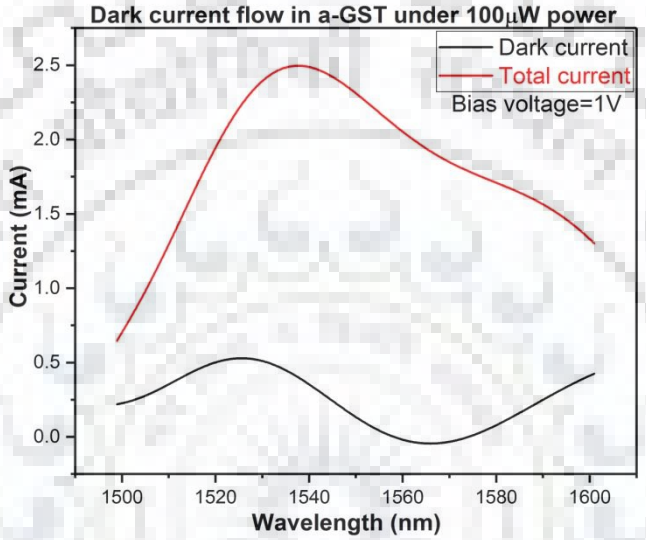

Figure 23 Dark current in a-GST

Similar, work is done for c-GST and the currents are plotted for comparison.

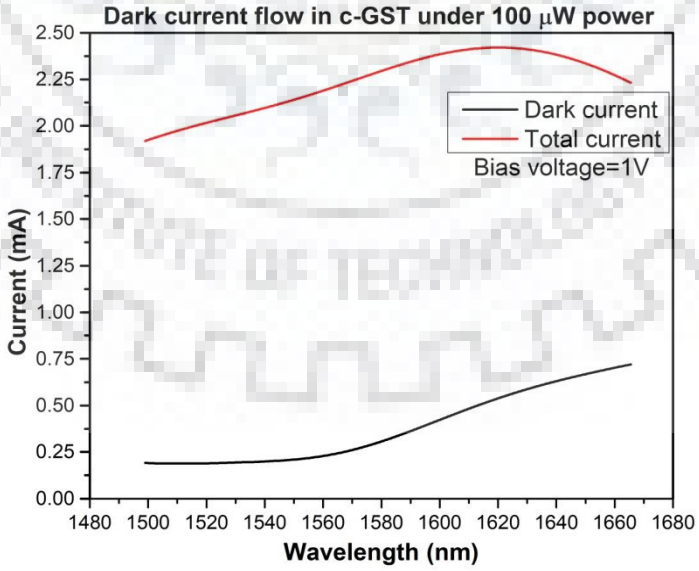

Figure 24 Dark current in c-GST

Since, we have put in the values of refractive index of a-GST at 1550nm so calculated current by simulation would be correct around 1550nm.

Unit 7: Observations and Conclusion

Now, the above plotted results is explained and analysed. In figure 13 and figure 14 plots are showing increase in current flowing through current monitor at input optical powers is increased. As more optical power is falling on detector more electron hole pairs are produced that will cause more photocurrent. For a-GST input power applied are 50μW, 100μW and 500μW and current at 1550 nm at these power is observed to be 4.2mA, 4.4mA and 5mA respectively. Also, for c-GST input power applied are 10μW, 100μW and 500μW and current at 2400nm at these power is observed to be 2.6mA, 6.4mA and 8.5mA respectively.

In figure 15 a-GST in supplied with 100μW optical power and bias voltage is changed from 1V 3V and 5V.Since more strong electric field in active region of detector means very perfect collection of electrons and holes at different electrodes with lesser possibility of recombination just after generation. So, as bias voltage increases carrier collection efficiencies at opposite electrodes increase with decrease in carrier transit time. Hence current increases with bias voltage increase. In comparison between figure 15 and figure 16 we observe that current level at same bias voltage in a-GST at 1550nm is higher than that at 2200 nm. Reason for the same is that energy of photon at 1550 nm wavelength (0.80 eV) is comparable to the band gap of a-GST (0.71eV) whereas energy at 2200nm (0.56 eV) is far less than band gap of a-GST. Similar analysis can be done for current plots shown for c-GST in figure 17 and figure 18.

From figure 19 to figure 22 biasing voltage has been set to 1V fixed and optical input power is varied to very large range to find out the typical value of minimum power that could be detected by the detector. As power varied from 1pW to 1mW and total current is measured through current monitor. Then dark current is also calculated and plotted in figure 23 and figure 24 for a-GST and c-GST respectively.

Some of the tables containing data points from the above plotted graphs are shown below and used to show some calculation of results, also other data points can be taken from plots and analysed in the similar way.

Power (P_{in})	Wavelength (λ)	Frequency (ν)	Phase	Current (I)	Volume loss in GST
10μW	1550 nm	193.5 THz	c-GST	0.95mA	$8x10^{-6}W$
10μW	2100 nm	142.7 THz	c-GST	1.44mA	$8.2x10^{-6}W$
10μW	1550 nm	193.5 THz	a-GST	0.90mA	$6.4x10^{-6}W$
10μW	2100 nm	142.7 THz	a-GST	2.81mA	$5.1x10^{-7}W$

Table 5 Analysis at 10μW power

Power (P_{in})	Wavelength (λ)	Frequency (ν)	Phase	Current (I)	Volume loss in GST
100μW	1550 nm	193.5 THz	c-GST	2.13mA	$8x10^{-5}W$
100μW	2100 nm	142.7 THz	c-GST	2.65mA	$8.2x10^{-5}W$
100μW	1550 nm	193.5 THz	a-GST	2.35mA	$6.4x10^{-5}W$
100μW	2100 nm	142.7 THz	a-GST	2.80mA	$5.1x10^{-6}W$

Table 6 Analysis at 100μW power

Power (P_{in})	Wavelength (λ)	Frequency (ν)	Phase	Current (I)	Volume loss in GST
1mW	1550nm	193.5 THz	c-GST	5.91mA	0.00080W
1mW	2100nm	142.7 THz	c-GST	6.53mA	0.00082W
1mW	1550nm	193.5 THz	a-GST	7.05mA	0.00064W
1mW	2100nm	142.7 THz	a-GST	5.31mA	0.00005W

Table 7 Analysis at 1mW power

Analysis of switchability:

When magnitude of current flowing in device is observed for switchability, current flowing in device at 1550 nm for a-GST must be same or comparable to the current flowing at 2100 nm for c-GST. This is true for the input powers of 100μW and 1mW. Here, the simulated detector could be considered as switchable but at 10μW current results could not show switchability as currents are not comparable at 1550nm and 2100nm. Some more analysis need to be done for justification of switchability at different powers. Till now power selective switchability is observed.

Calculation of Responsivity:

Responsivity, which is the most crucial parameter of a photodetector is the ratio of photocurrent produced to the input power given to the detector. It can be easily calculated now with the help of above data. Using eq. 2.5 and 2.13 from figure 23 and figure 24 we can calculate responsivity as follows:

- P_{in}= 100μW and c-GST at 1550nm

  I_D = 0.25mA, I = 2.10mA

  Now, I_p= I - I_D = 2.10 – 0.25 = 1.85mA (Photocurrent)

  $R = \frac{I_p}{P_{in}} = \frac{1.85\ X\ 10^{-3}}{100\ X 10^{-6}}$ = 18.5 A/W.

- P_{in} = 100μW and a-GST at 1550nm

  I_D = 0.10mA, I = 2.25mA

  Now, I_p = I – I_D = 2.25 – 0.10 = 2.15mA (Photocurrent)

  R= $\frac{I_P}{P_{in}} = \frac{2.15\ X\ 10^{-3}}{100\ X\ 10^{-6}} = 21.5$ A/W.

Here, some calculations on data taken from graphs are shown. Responsivity for 100μW power input is calculated as 18.5 A/W and 21.5 A/W for c-GST and a-GST respectively. Further calculations could be done by taking total current values from figure 19, 20, 21 and 22 by subtracting dark current value from total current and dividing by power used for simulation.

Future Scope

If I had to continue this project further or anyone else is interested in continuing this work. I would like to suggest for working on following parameters:

- Using different thin film technologies or structures to improve absorption.
- Length of GST can be increased further similar to waveguide photodetector to increase size of region of absorption.
- Gain factor increment
- Circuit implementation
- Fabrication

References

1. Bahram Jalali, And Sasan Fathpour, “Silicon Photonics”, Journal of Lightwave Technology, Volume 24.
2. Amnon Yariv and Pochi Yeh, “Photonics”, Oxford University Press, fourth edition.
3. Simon M. Sze, “Physics of semiconductor devices”, Wiley student edition.
4. Govind P.Agrawal, “Fiber-optic communication systems”, third edition.
5. Entezari, M. and Zavvari, M., 2016. Application of hyperbolic metamaterials for responsivity enhancement of thin film photo-conductive detectors. *IEEE Sensors Journal*, *16*(24), pp.8916-8920.
6. Burroughes, J.H. and Hargis, M., 1991. 1.3 mu m InGaAs MSM photodetector with abrupt InGaAs/AlInAs interface. *IEEE Photonics technology letters*, *3*(6), pp.532-534.
7. Srivastava, V., Tolani, M. and Kumar, R., 2018. Design and Simulations of $Ge_2Sb_2Te_5$ Vertical Photodetector for Silicon Photonic Platform. *IEEE Sensors Journal*, *18*(2), pp.540-546.
8. J. Robertson, K. Xiong, P. W. Peacock, “Electronic and atomic structure of $Ge_2Sb_2Te_5$ phase change material”, Thin solid films.
9. Kato, T. and Tanaka, K., 2005. Electronic properties of amorphous and crystalline $Ge_2Sb_2Te_5$ films. *Japanese journal of applied physics*, *44*(10R), p.7340.
10. Lee, B.S., Abelson, J.R., Bishop, S.G., Kang, D.H., Cheong, B.K. and Kim, K.B., 2005. Investigation of the optical and electronic properties of $Ge_2Sb_2Te_5$ phase change material in its amorphous, cubic, and hexagonal phases. *Journal of Applied Physics*, *97*(9), p.093509.
11. Woda, M., 2012. Electrical transport in crystalline phase change materials.
12. CST microwave studio 2016- workflow and solver overview.
13. Tsafack, T., Piccinini, E., Lee, B.S., Pop, E. and Rudan, M., 2011. Electronic, optical and thermal properties of the hexagonal and rocksalt-like Ge2Sb2Te5 chalcogenide from first-principle calculations. *Journal of Applied Physics*, *110*(6), p.063716.

Appendix

1. Plot for ε and ε' for hexagonal phase GST is shown below:

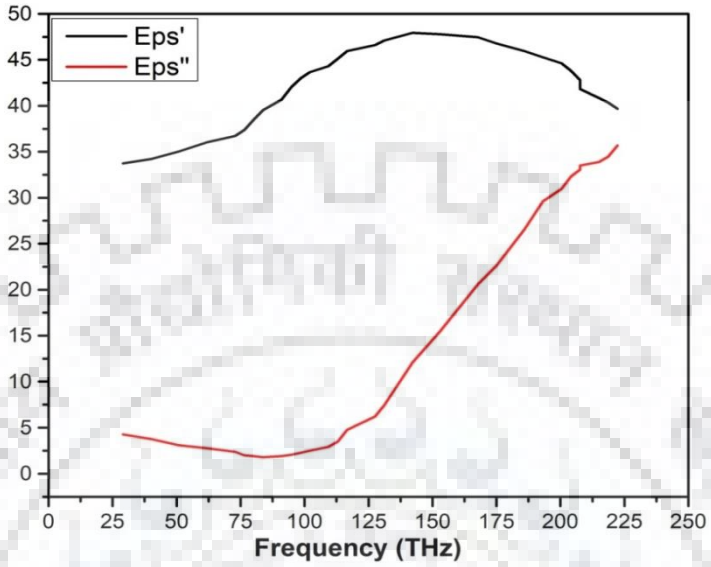

Figure 25

2. Table containing values of refractive index n (ω) and extinction coefficient k (ω) calculated from Maxwell model using ε and ε' values are shown below:

Frequency (THz)	Energy (eV)	n(ω)	k(ω)
100	0.414	7.247	1.793
105	0.434	7.247	1.814
110	0.455	7.263	1.846
115	0.476	7.263	1.878
120	0.497	7.279	1.905
125	0.517	7.279	1.947
130	0.538	7.311	1.964
135	0.559	7.295	2.038
140	0.579	7.311	2.081
145	0.601	7.311	2.129
150	0.621	7.326	2.177
155	0.641	7.326	2.209
160	0.662	7.326	2.279
165	0.683	7.340	2.391
170	0.704	7.342	2.434
175	0.724	7.407	2.455
180	0.745	7.439	2.503

Table 8 n & k values